energy&fuels

Article

pubs.acs.org/EF

Effect of the Fuel Injection Pressure on Particulate Emissions from a Gasohol (E15 and M15)-Fueled Gasoline Direct Injection Engine

Nikhil Sharma and Avinash Kumar Agarwal*

Engine Research Laboratory, Department of Mechanical Engineering, Indian Institute of Technology Kanpur, Kanpur, Uttar Pradesh 208016, India

ABSTRACT: Gasoline direct injection (GDI) engines have become popular in transportation sector off late and may possibly substitute diesel engines for various applications because of their superior power output and higher thermal efficiency. In this study, a single-cylinder, wall-guided GDI engine was investigated for its emission characteristics using a stoichiometric alcohol−gasoline mixture (gasohol) and air at 2000 rpm engine speed and 2.5−8.5 bar indicated mean effective pressure (IMEP). Gasoline blended with 15% (v/v) ethanol (E15), gasoline blended with 15% (v/v) methanol (M15), and gasoline as baseline fuel were the test fuels investigated for particulate matter (PM)/particulate number (PN) emissions in homogeneous charge mode of the GDI engine. The particle size number distributions were determined using an engine exhaust particle size analyzer (EEPS 3090, TSI) at two fuel injection pressures (FIPs, 80 and 120 bar). It was experimentally determined that FIP played a vital role in the fuel−air mixture preparation and affected particulate emissions significantly in a GDI engine. Particulate size-number, size-mass, and size-surface area distributions were reported for these test fuels under identical load conditions. PN emissions were quite high at lower IMEPs. It decreased at intermediate IMEP but increased at the highest IMEP tested. A trade-off between PM/PN was also observed. The experiment demonstrated that there is a need to control PM/PN emissions from a GDI engine in order to meet stringent emission norms. The count mean diameter gave clear statistical information that smaller particulate offers relatively higher surface area per unit mass of particulate, leading to higher adsorption of toxic compounds, making it possibly more toxic.

1. INTRODUCTION

Gasoline direct injection (GDI) engines are superior to conventional multi-point port fuel injection (MPFI) engines because of their inherent advantages, such as superior power output, greater fuel economy, lower emissions, smoother operation, and ability to accommodate alternate fuels.[1]

Particulate matter (PM) emissions from GDI engines pose serious concerns as a result of various health issues associated with them.[2−5] PM emissions are the most important negative aspect of internal combustion (IC) engines, especially GDI and compression ignition (CI) engines. Figure 1 shows the zones of human respiratory system affected by various sized PM. These PM emissions affect human health adversely[6] because they penetrate deep into the respiratory system (nasopharynx, trachea, bronchii, bronchioles, and alveoli)[7,8] during inhalation and contaminate it with toxic substances as they travel downstream (Figure 1). As PM size becomes smaller, the severity of their health impact increases because of the increased surface/volume ratio. Finer particles penetrate deeper into the lungs (Figure 1) and can eventually cross the cellular membranes[9] and finally enter the bloodstream. PM_{10} is largely filtered out in the nostrils, throat, and bronchial tubes. Some part of the $PM_{2.5}$ can, however, penetrate the bronchial tubes, and $PM_{0.1}$ can even reach up to the alveoli and invade the bloodstream. A few important health issues, which may lead to premature death,[10] as a result of PM emission include asthma, irregular heartbeats, decreased lung function, non-fatal heart attacks, and severe coughing. Hence, there is a need to understand reasons for PM formation in the engine and their effects on public health, using alternative fuels in an engine and ultimately control the PM formation.

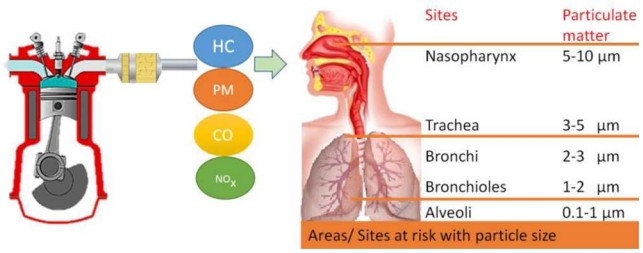

Figure 1. Journey of engine exhaust particulate into the human respiratory system.

Researchers are working across the globe to meet stringent emission norms from GDI engines, especially the PM emissions.[11−14] Fuels for GDI engines are constantly evolving over time because of scientific and economic needs of the society.[15−17] Soot is mainly formed in the engine combustion chamber by partial or incomplete combustion. Pyrolytic reactions occurring in the absence of oxygen produce pyrolyzed hydrocarbon (HC) compounds, such as ethyne. This acts as a precursor for formation of polycyclic molecules (ring or aromatic compounds), which ultimately lead to the formation of particulate. Yinhui et al.[18] investigated primary particulate emissions, including mass, number, size distributions, etc., from

Received: November 1, 2016
Revised: February 3, 2017
Published: March 14, 2017

DOI: 10.1021/acs.energyfuels.6b02877
Energy Fuels 2017, 31, 4155−4164

a GDI engine fueled with gasoline−alcohol blends. They reported that 10% (v/v) ethanol blended with gasoline increased particulate emissions at low loads. The higher the aromatic content of the gasoline, higher were the PM/particulate number (PN) emissions. Reducing the olefin content in gasoline reduced the PM and PN emissions at higher loads. Wang et al.[19] compared the impact of ethanol and gasoline on PM emissions in a single-cylinder GDI research engine and reported that ethanol yielded lower PM emissions because of its relatively higher volatility and oxygen content. They reported that, as a result of higher atomization and fuel injection pressure, particulate emissions decreased. A trade-off between PM and PN emitted from GDI engine was also observed, irrespective of the test fuel used. Cho et al.[20] reported that emission characteristics of a GDI engine were significantly influenced by blending ethanol with gasoline. Ethanol (20%) blended with gasoline reduced PN emissions by up to 96%. The authors also reported that both higher fuel injection pressure (FIP) and higher ethanol concentration blended with gasoline reduced the PN emissions. Lue et al.[21] investigated the effect of ethanol−gasoline blends on PM/PN from a GDI engine and reported that ethanol−gasoline blends (gasohols) increased the PN concentration at lower loads and vice versa at higher loads. Wang et al.[22] also investigated particulate emissions from a GDI engine equipped passenger car, operating under the New European Driving Cycle (NEDC). They reported that gasohols reduced tailpipe PM emissions by 33.2−40.2%. Vancoillie et al.[23] experimentally evaluated potential emission reduction benefits by blending methanol with gasoline and reported that methanol could be used as an alternative fuel with efficiencies similar to diesel engine, however, with relatively lower emissions than gasoline in a GDI engine. Chen et al.[24] reported that an increase in ethanol addition to gasohol led to an increase in both PM/PN emissions from a cold engine. Lattimore et al.[25] reported that butanol blended with gasoline was an effective way to reduce PN emissions. They concluded that among (i) 20% (v/v) ethanol blended with gasoline (E20), (ii) 20% (v/v) butanol blended with gasoline (Bu20), and (iii) baseline gasoline, Bu20 showed the best potential to reduce PM emissions and also exhibited the best combustion characteristics.

European emission legislation for PN imposes a limit on the GDI engine cars to emit $<6 \times 10^{12}$ particles/km [World Economic Forum (WEF)]. This legislation would become more stringent from September 2017, and the PN limit would be further reduced to $<6 \times 10^{11}$ particles/km.[26] Optimized FIP, fuel injection timing, and use of alternative fuels have the potential to reduce PN emissions, which, in turn, will be less harmful for public health. FIP also exhibits a significant effect on regulated gaseous emissions, such as HC, oxides of nitrogen (NO_x), and carbon monoxide (CO). Zhang et al.[27−29] used a selective catalytic reaction system to reduce NO_x emissions from a diesel engine. Price et al.[30] investigated the effect of blending alcohol with gasoline on particulate emissions (PN and PM) and HC emissions from a GDI engine. Authors also plotted distillation curves for M30, E30, M85, E85, and gasoline. It was found that, for rich mixtures, the number of accumulation mode particles reduced and the number of nucleation mode particles increased in oxygenated fuels. Among test fuels, E85 exhibited the lowest PN emissions. Unleaded gasoline, E30, and M30 showed similar trends; however, the highest PN emissions were measured for M85. Particulate size distribution was highest for M85 and gasoline showed the smallest size accumulation mode particles amongst all test fuels. As the fuel injection timing was retarded, accumulation mode particles increased for unleaded gasoline and E30. However, for M30, M85, and E85, PM emissions were almost identical. The higher was the evaporation rate of test fuel, the lower was the possibility of fuel droplet striking on the piston top and the cylinder walls. Compression also enhances the evaporation rate of the fuel droplets.

In Europe and the U.S.A., GDI engine technology continues to capture an increasing share in the automotive segment. The GDI engines have to comply with upcoming stringent emission norms (Euro 6c) without altering the current engine technology. In such a scenario, gasoline particulate filters (GPFs) in the after-treatment systems are considered to be an enabling technology for achieving desired PM and PN emission reduction.[31−33] GPF development has been investigated in a number of studies.[34−36]

In this study, comparative evaluation of 15% (v/v) ethanol and methanol blended with gasoline (E15 and M15, respectively), i.e., gasohols for PM and PN emissions, has been performed under steady-state engine operating condition in homogeneous charge mode in the GDI engine at two FIPs (80 and 120 bar) and five engine loads. This study provides valuable insights of particulate size-number, size-mass, and size-surface area distributions for engine loads varying from 2.5 to 8.5 bar indicated mean effective pressure (IMEP), while using gasohols. Count mean diameter (CMD) of particulate was calculated from the observed particulate characteristics, which gave very clear statistical information on the PN emissions with increasing engine load. Engine performance characteristics and regulated gaseous emissions, such as total hydrocarbons (THCs), CO, and NO_x, were also measured for all test fuels and test conditions.

2. EXPERIMENTAL SECTION

Fuel properties play a critical role in determining overall emission characteristics. Table 1 shows various fuel properties of gasoline and alcohols.

The experimental setup consists of a 500 cc, single-cylinder GDI research engine (HMC Seta 0.5 L, Mobiltech), which delivered a rated torque of 30 N m at 2000 rpm. Specifications of the test engine are given in Table 2. The test engine was coupled with a 36 kW transient AC dynamometer (6-2013, Dynomerk Controls). Figure 2 shows the schematic of the experimental setup. An optical crank angle encoder (365C, AVL) was attached to the crankshaft, which delivered 720 pulses in every revolution. This encoder was attached to a four-channel, high-speed combustion data acquisition and analysis system (Indi-micro, AVL) through a signal conditioning unit (365-C, AVL). An indicating spark plug (ZI31_Y5S, AVL) was mounted on the engine cylinder head, and its output of in-cylinder pressure signals was provided to the combustion analyzer, via an in-built charge amplifier. Two surge tanks, one each for inlet and outlet, were attached to the air inlet and exhaust from the engine. The function of these surge tanks was to dampen the oscillations created by pulsations as the air was sucked/exhausted in one of the four strokes of the engine cycle. A fully programmable open electronic control unit (ECU; m400, MOTEC) was attached to the GDI engine, and it controlled the fuel injection timing, spark timing, and injector pulse width, depending on the operational requirement. The injector peak and hold driver (ZB-5100G, Zenobalti) was attached to the engine through the open ECU, which received trigger signal from the optical encoder.

An engine exhaust particle sizer (EEPS-3090, TSI Inc.) was used for particulate size-number, size-mass, and size-surface area distributions of the soot emitted from the test engine. In addition, engine oil, coolant, and fuel conditioning units (fuel system compact, AVL) were connected to the test engine. Regulated gaseous emissions, namely,

DOI: 10.1021/acs.energyfuels.6b02877
Energy Fuels 2017, 31, 4155−4164

Table 1. Test Fuel Properties

fuel property	unleaded gasoline	ethanol	methanol
molecular formula	C_4–C_{12}	C_2H_5OH	CH_3OH
adiabatic flame temperature (°C)	2138	1920	1870
boiling point temperature/range (°C)	25–215	78.4	64.5
cetane number	15	8	3
density at 20 °C (g/cm^3)	0.745	0.79	0.796
flammability limit (vol %)	7.6	3.3–19	36
flash point (°C)	from −45 to −38	8	12
hydrogen content (wt %)	13.59	13.1	12.5
kinematic viscosity at 40 °C (mm^2/s)	0.494	1.221	0.596
laminar flame speed (m/s) (λ = 1)	0.38	0.4	0.523
latent heat of vaporization (kJ/kg)	310–320	920	1100
lower heating value (MJ/kg)	42.7	26.8	19.9
molecular weight (kg/kmol)	110	46	32.042
oxygen content (wt %)	<0.05	34.8	50
research octane number	95	108.6	108.7
stoichiometric air/fuel ratio	14.7	9.02	6.49
sulfur content (wt %)	ultra low	0	0
viscosity at 40 °C (mm^2/s)	0.4–0.8	1.08	0.59
surface tension at 27 °C ($\times10^{-3}$, N/m)	18.93	22.05	22.18
vapor pressure at 27 °C (MPa)	0.045–0.09	0.018	0.032
ignition limit (vol %)	1.4–7.6	4.3–19	6.7–36

Table 2. Engine Specifications

engine type	single-cylinder GDI engine
bore/stroke (mm)	86/86
displacement volume (cm^3)	500
connecting rod length (mm)	196
compression ratio	10.5
maximum power at 3000 rpm (kW)	10
maximum torque at 3000 rpm (N m)	32
number of injector holes	6

CO and NO_x, were measured using the non-dispersive infrared (NDIR; MEXA-584L, Horiba) analyzer, and THCs were measured using a hot flame ionization detection (HFID) analyzer (MEXA-1170HFID, Horiba). The response time of the detector was < ±1.5 s for switching between zero line and span line for calibration, and its repeatability was < ±1.0% of the full scale.

Experiments were performed on the GDI engine fueled by M15, E15, and baseline gasoline (G100). For each test fuel, exhaust gas samples were drawn from the engine tail-pipe after steady-state condition was achieved. To achieve a thermally stable condition, the test engine was operated at a particular load/speed combination for 10 min prior to measurements.

Technical specifications of particulate measurement system (EEPS) are given in Table 3. EEPS has the ability to measure particle sizes

Table 3. Technical Specifications of EEPS 3090

particle size range (nm)	5.6–560
particle size resolution (channels per decade)	16 (32 in total)
electrometer channels	22
charger mode of operation	unipolar diffusion charger
inlet cyclone 50% cut-point (μm)	1
maximum data rate (Hz)	10

ranging from 5.6 to 560 nm with a maximum concentration of 10^8 particles/cm^3 of exhaust. It has a size resolution of total 32 channels. Because the PN concentration in raw exhaust emitted from the GDI engine was much higher than the measuring range of EEPS, raw exhaust was diluted 560 times using sheath air supplied by a rotating disk thermodiluter (MD19-2E, Matter Engineering AG). Thus, the concentration of particles in diluted exhaust comes in the measurable range, and these values were later multiplied by the dilution factor, to obtain the concentration of PM emanating from the engine tailpipe.

Measurements were taken for 60 s at a frequency of 1 Hz at each test condition. The graphs presented in the Results and Discussion section were drawn from an average data set of 60 measurements, and the error bars were shown corresponding to the standard deviation of a particular data set. The entire measurements were performed according to Indian Standard IS/ISO 8178-4.[37] The particulate size number distribution was calculated using the following formula:

$$n = \frac{c}{tQ}\frac{\varphi}{\eta}$$

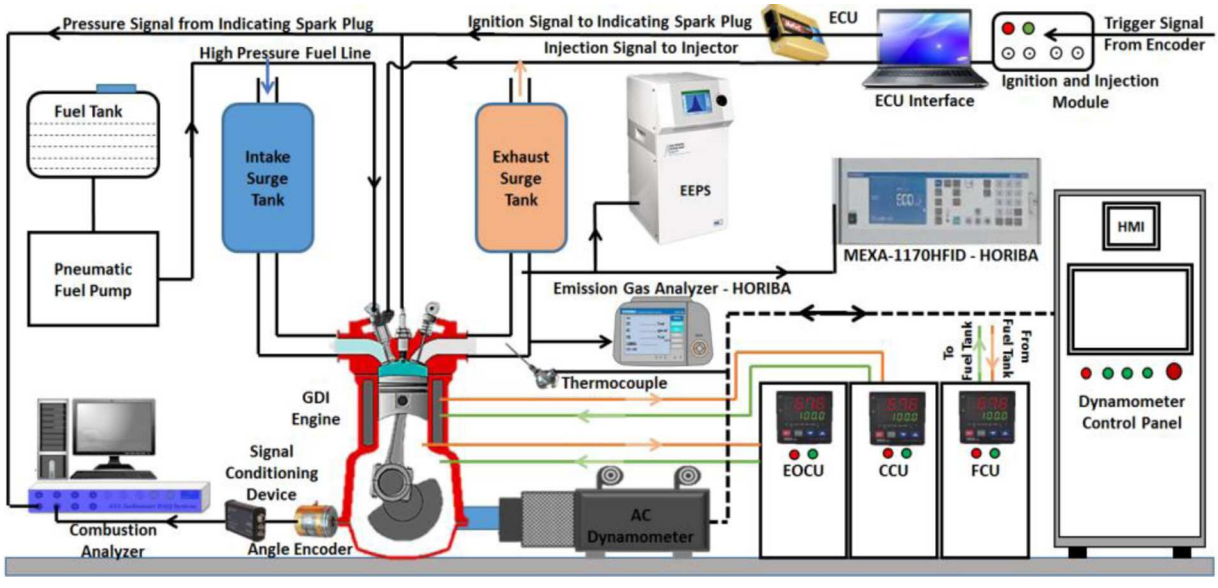

Figure 2. Schematic of the engine experimental setup.

DOI: 10.1021/acs.energyfuels.6b02877
Energy Fuels 2017, 31, 4155–4164

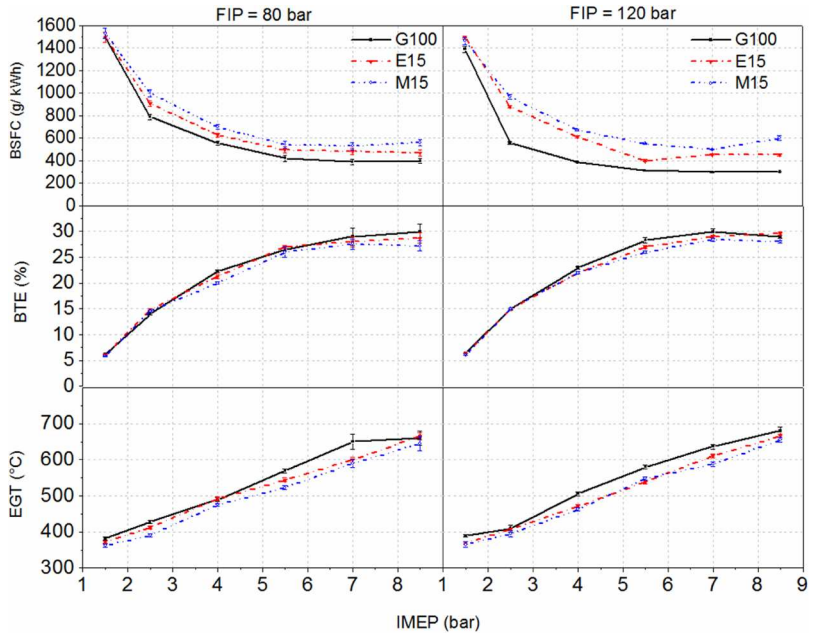

Figure 3. EGT, BTE, and BSFC variations with IMEP at 120 bar FIP.

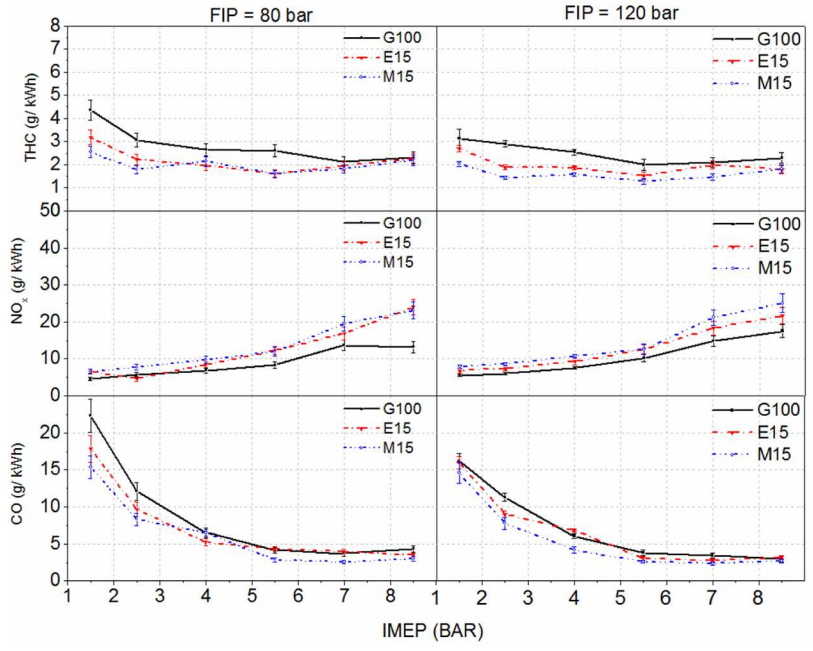

Figure 4. Mass emissions of CO, NO_x, and THCs with varying IMEP.

where n is the number weighted particle concentration per channel, c is the particle count per channel, φ is the exhaust dilution factor, t is the sampling time, Q is the sample flow rate, and η is the sample efficiency factor per channel.

The PM size distribution was calculated by the following formula:

$$m = \rho v$$

where m is the mass-weighted concentration per channel, ρ is the particle density, and v is the volume-weighted concentration per channel.

The particulate size surface area distribution was calculated by the following formula:

$$s = \pi D_p^2 n$$

where s is the surface-area-weighted concentration per channel, D_p is the particle diameter (channel midpoint), and n is the number-weighted concentration per channel.

Total PN distribution was calculated by the following equation:

$$N = \sum_{l}^{u} n$$

where N is the total number concentration, l is the lower channel boundary, u is the upper channel boundary, and n is the number-weighted concentration per channel.

The fuel temperature was maintained at 20 °C throughout the experiment with the help of the fuel conditioning unit. The temperature and pressure of the lubricating oil were maintained at

DOI: 10.1021/acs.energyfuels.6b02877
Energy Fuels 2017, 31, 4155−4164

90 °C and 3.5 bar, respectively, using the lubricating oil conditioning unit.

3. RESULTS AND DISCUSSION

This experimental investigations provides detailed insights of the particle size-number distribution emitted from the GDI engine fueled with gasohols and baseline gasoline at two FIPs and five engine loads and their potential health implications. Engine performance characteristics along with gaseous emissions were measured for all three test fuels and are shown in Figures 3 and 4, respectively. Figure 3 shows variations in the exhaust gas temperature (EGT), brake thermal efficiency (BTE), and brake-specific fuel consumption (BSFC) with IMEP for the three test fuels at 2000 rpm and FIP of 80 and 120 bar.

From Figure 3, it can be observed that, as IMEP increases, EGT also increases. EGT was relatively higher at FIP of 120 bar. BTE reached maximum values of ∼27.1% (G100), ∼28.7% (E15), and ∼29.8% (M15) at 80 bar FIP and ∼28.0% (G100), ∼29.6% (E15), and ∼29.0% (M15) at 120 bar FIP. BTE of gasohols was found to be higher than that of baseline gasoline because of the presence of fuel oxygen. BTE for 120 bar FIP was relatively higher than that for 80 bar FIP. BSFC decreased from ∼1494 g/kWh at no load to ∼398 g/kWh at full load at 80 bar FIP and from ∼1388 g/kWh at no load to ∼300 g/kWh at full load at 120 bar FIP. BSFC for the gasohols was higher than baseline gasoline. This was because the energy content (LHV) of gasohols was relatively lower than baseline gasoline; therefore, higher fuel quantity per engine cycle was injected in order to achieve the same torque output from gasohols.

Figure 4 shows the variations in regulated gaseous mass emissions (g/kWh) at FIP of 80 and 120 bar at 2000 rpm engine speed. CO is a product of incomplete combustion in the combustion chamber. CO emission decreased with increasing IMEP because the fuel/air ratio was maintained constant throughout the experiments, which lead to more complete combustion in the entire range of engine load (IMEP). CO was in the range of 22.3−2.9 g/kWh for all test fuels at 80 bar FIP. However, at 120 bar FIP, a relatively lower CO emission in the range of 16.1−2.9 g/kWh was observed. NO_x emissions increased with an increasing engine load, irrespective of the test fuel used. The oxygen content of gasohols leads to more complete combustion, which increases the peak in-cylinder temperature. NO_x formation in an engine cylinder is a highly temperature-dependent phenomenon. NO_x formation increases with an increase in peak in-cylinder temperature; therefore, NO_x emissions were higher from the oxygenated fuels, namely, gasohols. NO_x emissions were relatively higher at 120 bar FIP. THC emissions decreased with an increasing engine load. THC formation takes place as a result of flame quenching near the combustion chamber walls, which results in partial burning of fuel molecules. THC emissions were relatively lower from gasohols at 120 bar FIP.

3.1. Particulate Size-Number Distribution. PM from the GDI engine are primarily formed as a result of fuel impingement on the cylinder walls and piston top. This results in incomplete fuel vaporization and incomplete fuel−air mixing, resulting in pockets of rich fuel−air mixtures. Figure 5 shows the particle size-number distributions for E15, M15, and baseline G100 as a function of IMEP at 2000 rpm with 80 and 120 bar FIP. Particulate emissions were relatively higher for both gasohols at lower IMEP in comparison to baseline gasoline. Gasohols resulted in a higher unburnt HC

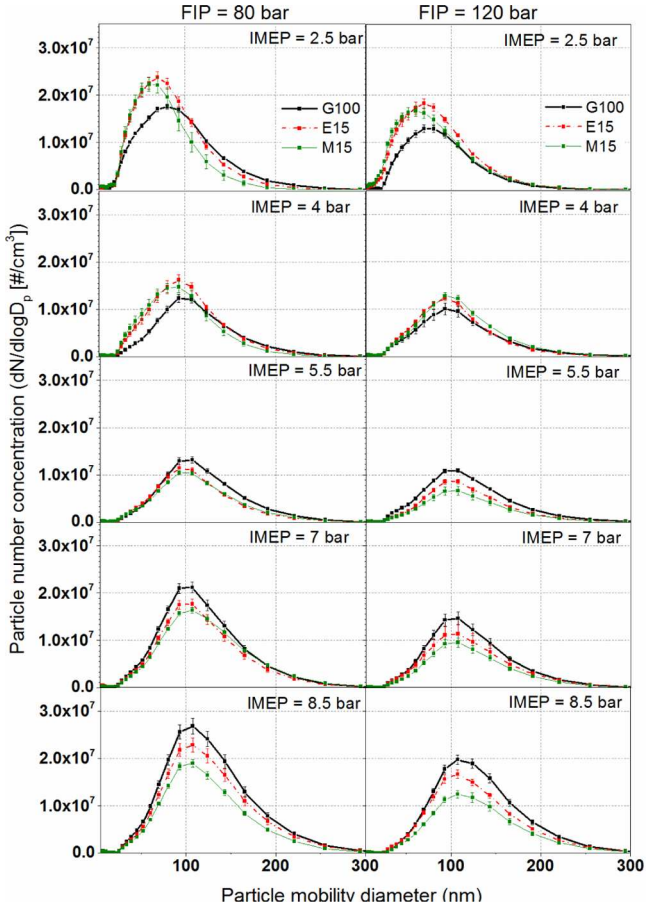

Figure 5. Particulate number versus particulate mobility diameter (nm) at FIPs of 80 and 120 bar.

concentration as a result of lower in-cylinder temperatures at lower engine loads. PN emissions were quite high at 2.5 bar IMEP, which decreased with an increasing engine load up to IMEP of 5.5 bar at both FIPs. At lower IMEP (2.5−5.5 bar), the exhaust gas temperature was relatively lower (Figure 3), which led to higher particulate formation, possibly as a result of higher degree of incomplete combustion. Similar observations are reported in the literature as well.[18,21,24] With an increasing engine load, particulate size-number distribution shifted toward larger particle sizes (D_p ∼ 100 nm). As IMEP increased from 5.5 to 8.5 bar, PN emission further increased and EGT reached a certain level (Figure 3), where particulate oxidation began, resulting in reduction in PN from gasohols. In addition, as IMEP increased from 5.5 to 8.5 bar, fuel injection quantity also increased. The resulting richer fuel−air mixture enhanced the degree of incomplete combustion, which increased PN at higher IMEP. It was also noted that the peak of PN emission shifted towards lower diameters (left) at lower IMEP.

Finer PM can penetrate deeper into human respiratory system upon being inhaled. These smaller particles emitted at lower loads will have higher retention in the alveolar region of lungs, and they easily transport toxic polycyclic aromatic hydrocarbons (PAHs) deep into lungs. Children are especially vulnerable to ill effects of air pollution because their respiratory and immune systems are immature and are at the stage of rapid development.[38] Children also inhale more air per unit body weight; therefore, their exposure is significantly higher to pollutants than adults. Chronic respiratory effects linked to

DOI: 10.1021/acs.energyfuels.6b02877
Energy Fuels 2017, 31, 4155−4164

ambient pollutant particles include reduced lung function and increased symptoms of bronchitis in both children and adults.[39−42]

Lower engine load contributes more toward PN and has negligible contribution to total particulate mass (Figure 6).

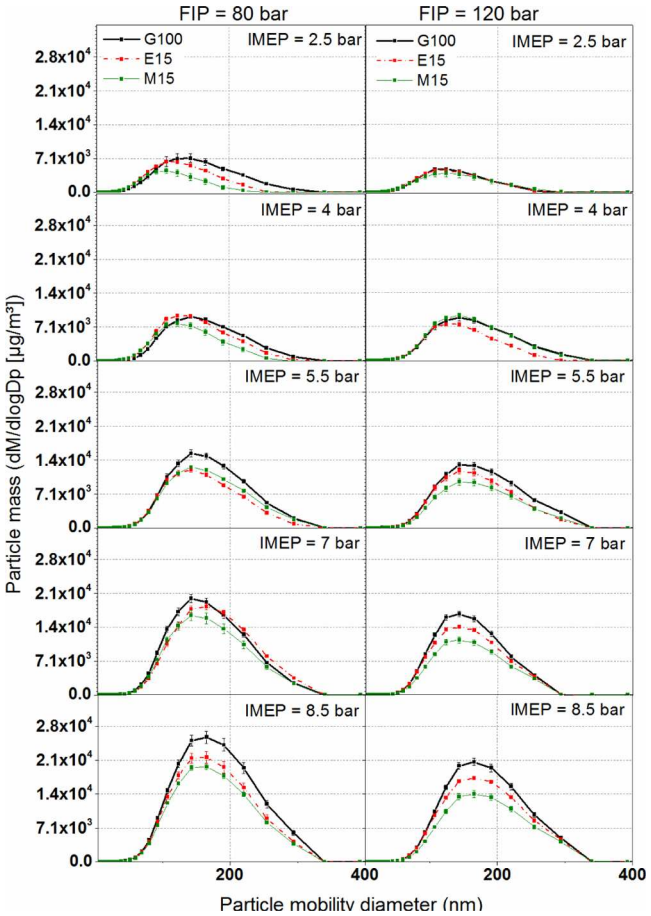

Figure 6. Particle size-mass versus particulate mobility diameter at FIP of 80 and 120 bar.

However, at higher IMEP, PN emissions from baseline gasoline were relatively higher compared to gasohols (M15 and E15). These observations were in agreement with the results reported in the literature.[19,24] Both gasohols emitted relatively lower PN at higher IMEP because of higher oxygen content, lower boiling point, lower carbon/hydrogen ratio, and higher octane number of gasohols compared to baseline gasoline. At higher IMEP, a higher quantity of fuel-borne oxygen leads to lower elemental carbon (EC) formation particularly from gasohols. The oxygen content of gasohols improves the combustion efficiency of the charge. Oxygen present in both gasohols improved the combustion by locally altering the fuel−air ratios. The octane numbers of methanol and ethanol were also higher than baseline gasoline. The laminar flame speeds of methanol and ethanol were approximately twice as fast as gasoline, which increased the heat release rate, resulting in superior combustion phasing.

The gasohols have a relatively higher latent heat of vaporization; therefore, they absorb greater amount of heat generated by combustion and from the intake manifold. Because of the presence of oxygen in the molecular structure of ethanol and methanol, blending them with gasoline decreases the peak combustion temperature at lower IMEPs. PM emissions from both gasohols have a higher organic volatile content compared to baseline gasoline, primarily as a result of reduction in elemental carbon formation by combustion of ethanol/methanol. Also, when ethanol/methanol is blended with gasoline, the soot precursor concentration reduces. This is because of the absence of aromatic components in ethanol/methanol, which are responsible for soot formation. Fuel-borne oxygen assists in attaining a higher degree of oxidation of unburnt and pyrolyzed HCs.

3.2. Particulate Size Mass Distribution. Particle size number distributions were used to calculate particle size-mass distributions for different test fuels. PM mostly comprises of agglomerates; however, it has been shown in the literature that they can be assumed to be spherical with a density of 1 g/cm^3 for calculating size-mass distribution with acceptable accuracy.[43−45]

Figure 6 showed the particle size-mass distributions for E15, M15, and G100 with an increasing IMEP at 2000 rpm at FIP of 80 and 120 bar. Larger diameter particles contribute more toward mass. Particle size-mass distributions showed that gasohols generated relatively lower PM emissions at lower IMEP. This was because the size-number distribution of particulate at lower IMEP was relatively lower. However, at higher IMEP, the particulate size generally increases; hence, they contribute to relatively higher particulate mass emission. It was also observed that, at higher IMEP, both gasohols had relatively lower particulate mass emissions compared to baseline gasoline. The PM emissions were relatively lower at FIP of 120 bar in comparison to FIP of 80 bar. Particulate with a higher mass will have a lower atmospheric retention time and will settle in relatively lesser time compared to lighter particulate.

It can be concluded from this study that gasohol origin particulate were relatively lighter in comparison to gasoline origin particulate; therefore, there is a possibility of them being relatively more toxic compared to gasoline origin particulate.

3.3. Particle Size-Surface Area Distribution. Figure 7 shows the particle size-surface area distributions for E15, M15, and G100 with increasing IMEP at 2000 rpm at FIP of 80 and 120 bar. Spray characteristics play a critical role in PM formation as well as control.[46,47] Agarwal et al.,[48] and Heywood[49] discussed particulate formation process in detail. During combustion, higher molecular weight HCs convert into smaller HCs, such as butadiene and acetylene, via the process of fuel pyrolysis in the engine combustion chamber. This process takes place at 2000−2400 K under deficient oxygen conditions. After some time, the temperature in the combustion chamber falls and nucleation mode particles coagulate together into a bunch of particles with sizes ranging from 70 to 100 nm. The particle surface area further increases by surface growth and spatial growth through PAH condensation, adsorption, and coagulation processes. In due course of time, the particulate surface area/volume increases because of them sticking together. Finally, the particles collide with each other and form agglomerates of a larger size and irregular shape. PM also increases wear of vital engine components.[50]

The size-surface area distribution tends to increase with increasing IMEP. Organic carbon (OC) mainly comprises of HCs, which do not burn during combustion and primarily originate from fuel or lubricating oil. OC is formed by condensation of hydrocarbon vapors formed as a result of incomplete combustion. Size-surface area distributions for both

DOI: 10.1021/acs.energyfuels.6b02877
Energy Fuels 2017, 31, 4155−4164

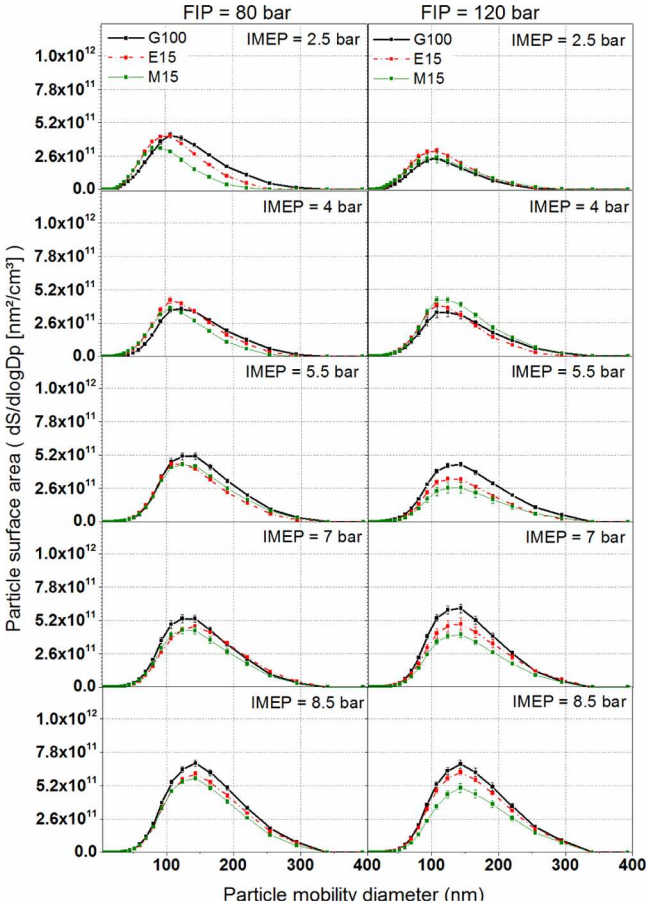

Figure 7. Particulate size surface area versus particulate mobility diameter (nm) at FIP of 80 and 120 bar.

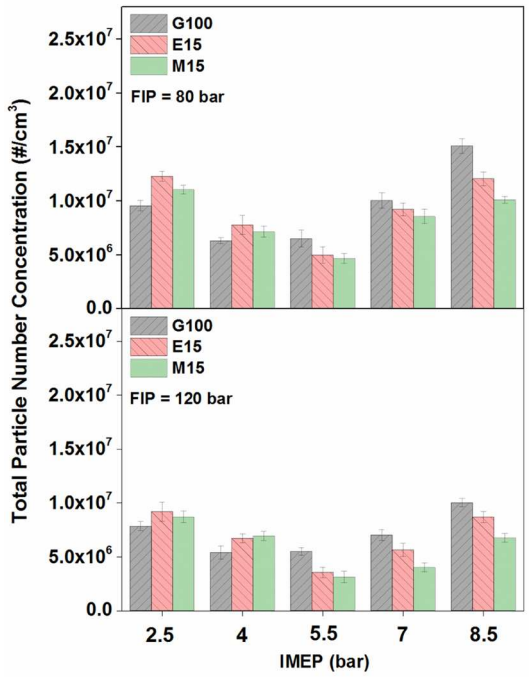

Figure 8. Total particulate number concentration with increasing IMEP at FIP of 80 and 120 bar.

gasohols were relatively higher at lower IMEP but decrease at higher IMEP compared to baseline gasoline. Organic compounds adsorbed on agglomerate surfaces may penetrate deeper into the bloodstream and can be potentially carcinogenic. The larger the size-surface area distribution of particulate, higher will be the probability of these combustion-generated PAHs to get adsorbed onto agglomerate surface and cause greater health hazard.

3.4. Total Particulate Number Distribution. Figure 8 shows the total PN concentration with increasing IMEP for E15, M15, and G100 at 2000 rpm at FIP of 80 and 120 bar. It is observed that the total PN concentration decreased from 2.5 to 5.5 bar IMEP and then increased up to 8.5 bar IMEP for all test fuels. The difference in total PN concentrations at varying IMEPs was probably due to the difference in peak combustion chamber temperatures for different test fuels. Consumption of lubricating oil at all IMEP at a constant engine speed of 2000 rpm was the same, however despite differences, the in-cylinder temperature for different test fuels was enough to pyrolyse the lubricating oil and form particulate. Lubricating oil contributes to formation of small as well as large particles.[51] It is observed that the total PN concentrations were relatively lower at FIP of 120 bar in comparison to FIP of 80 bar. It is desirable to have lower total PN emissions in the environment; therefore, higher FIP performs superior in a gasohol-fueled GDI engine.

3.5. CMD and Total Particulate Number Distribution. For comparison of the average particle size at a particular operating load, CMD was calculated and plotted against the total particulate number. CMD gives a better estimate of the adverse health effects of engine out particulate compared to total PN emission. It is not desirable to have a higher number of particles of smaller size, which can easily penetrate deep into the human respiratory system via inhalation and contaminate the respiratory system with toxic components adsorbed onto the agglomerate surfaces.

Figure 9 shows that CMD was the highest at 100% load for all test fuels. This clearly showed that higher engine loads resulted in emission of larger particulate. Also, the total particulate number concentrations at no load and full load were nearly identical; however, CMD at no load was significantly lower. Total PN concentrations were lower at FIP of 120 bar in comparison to FIP of 80 bar for all test fuels. It is desirable to have a lower total PN concentration; however, if the CMD is smaller, then it indicates a greater availability of surface area per unit mass of PM for adsorption of toxic compounds, which makes it relatively more toxic and undesirable.

3.6. Correlation between the PN and PM. Smaller particles contribute less to PM and more toward PN. On the other hand, larger particles contribute more to PM and less toward PN. A higher number of smaller particles will have a larger surface area available for adsorption of toxic species compared to a lower number of larger particles for the same PM mass. A higher particulate surface area available will adsorb higher quantity of toxic organic compounds. Hence, it is desirable to establish a relationship/correlation between the PN and PM emissions. Figure 10 shows the representation of such a relationship. PM is shown in the abscissa, and PN is shown in the ordinate. A lobe was plotted by joining particle sizes ranging from 5.6 to 560 nm in an increasing order. The larger PN and PM emission is reflected by a larger lobe. The significance of this graph lies in the fact that if the lobe is inclined toward the ordinate, this indicates higher PN dominance. On the other hand, if this lobe is inclined toward the abscissa, it indicates higher PM dominance. This lobe clearly shows that a smaller particle sizes with a larger PN will not contribute to mass

DOI: 10.1021/acs.energyfuels.6b02877
Energy Fuels 2017, 31, 4155−4164

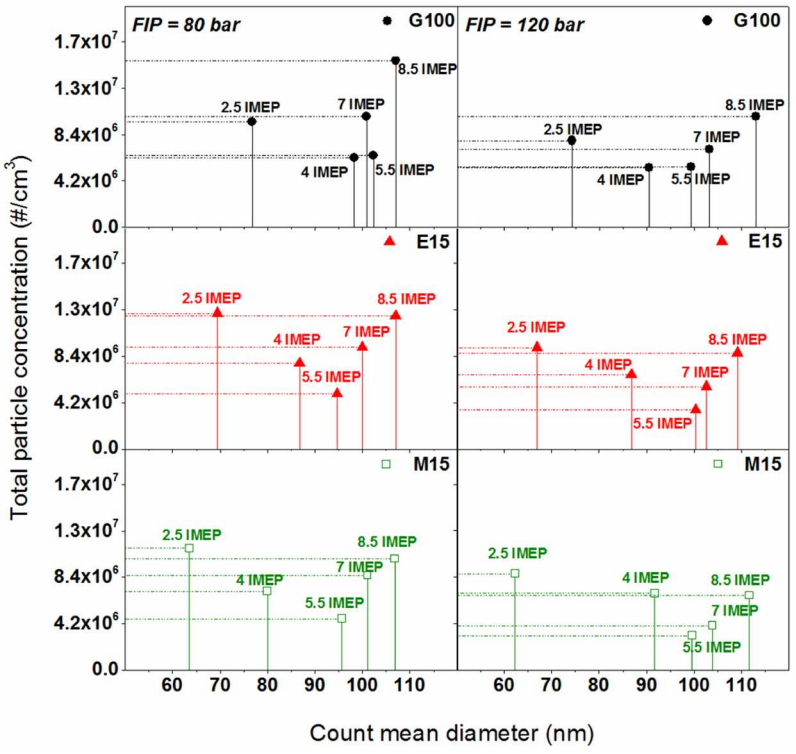

Figure 9. Variation of CMD with the total particulate number at FIP of 80 and 120 bar.

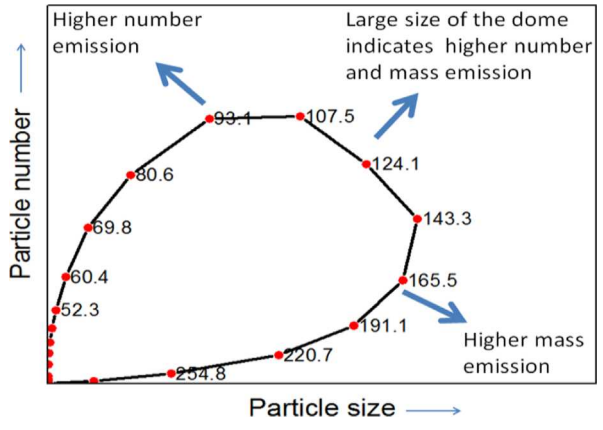

Figure 10. Explanation of correlation between PN and PM emissions.

measurement significantly and vice-versa. Increasing the size of the lobe indicates higher particulate emission (PM or PN).

Efforts have been made to establish correlation between PN and PM for this study in Figure 11. The size of the lobe was small at no load and was relatively more inclined toward the ordinate (showing PN dominance) for gasohol. As the engine load increased, the lobe tilted toward the abscissa, indicating increasing PM emissions with increasing engine load. For IMEP = 2.5 and 4 bar, the gasohol lobes were relatively smaller; however, at intermediate and high loads, the gasoline lobe was larger than those of gasohols. This indicated that gasohols emitted relatively more PN than gasoline at lower loads as a result of a relatively lower in-cylinder temperature, and as engine load increased, PN from gasohols decreased in comparison to gasoline. At higher engine loads, size and mass of particles increased for all test fuels. However, the lobes were relatively smaller for 120 bar FIP compared to 80 bar FIP.

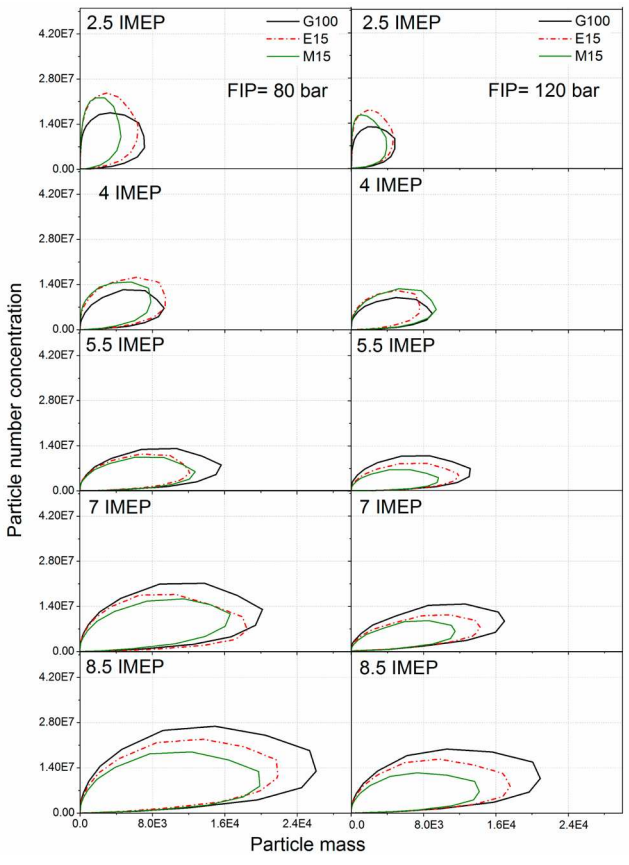

Figure 11. Correlation between PN and PM emissions from a gasohol-fueled GDI engine.

Larger lobes at higher engine loads indicated higher number emissions (PM/PN) for all test fuels.

DOI: 10.1021/acs.energyfuels.6b02877
Energy Fuels 2017, 31, 4155−4164

4. CONCLUSIONS

These experimental investigations have shown that gasohol blends emitted relatively higher PN emissions than baseline gasoline at lower engine loads in a GDI engine in homogeneous charge mode. At higher engine loads, gasohols emitted relatively lower PN emissions than baseline gasoline. PN emissions first decreased when the engine load increased from lower loads to intermediate loads but increased at higher engine loads, irrespective of the test fuel. PN emissions for FIP of 120 bar were an order of magnitude lower than that of FIP of 80 bar for all test fuels.

Total particle concentrations for no load and full load were nearly similar; however, CMD at no load was significantly smaller for all test fuels. CMD showed that smaller particles offered higher surface area per unit mass of PM for adsorption of heavier hydrocarbons, which may be potentially toxic. Size-surface area distributions of particulate emitted from gasohols were relatively higher compared to baseline G100 at lower IMEP and decreased at higher IMEP. The size surface area distribution of particulate increased with increasing IMEP for all test fuels. Particulate with a higher surface area per unit mass were potentially more toxic. Use of gasohols at lower loads does not offer any advantage in terms of PN emissions; however, at higher engine loads, PN emissions decreased significantly from gasohols compared to baseline gasoline in a GDI engine. This trend of PM and PN emissions can be accounted for while designing an engine or calibrating the GDI engine ECU for a particular application, because the PN limits are going to be enforced in most emission legislations worldwide.

AUTHOR INFORMATION

Corresponding Author

*E-mail: akag@iitk.ac.in.

ORCID

Avinash Kumar Agarwal: 0000-0002-7777-785X

Notes

The authors declare no competing financial interest.

ACKNOWLEDGMENTS

The authors acknowledge the equipment grant received from the Committee for the Acquisition of Research Equipment (CARE), Indian Institute of Technology Kanpur. Assistance of laboratory staff Roshan Lal and Surendra Singh during the experiments at the Engine Research Laboratory, Indian Institute of Technology Kanpur, is gratefully acknowledged.

NOMENCLATURE

Bu20 = 20% (v/v) ethanol blended with 80% (v/v) gasoline
E15 = 15% (v/v) ethanol blended with 88% (v/v) gasoline
ECU = electronic control unit
EEPS = engine exhaust particle sizer
EGT = exhaust gas temperature
FIP = fuel injection pressure
G100 = unleaded gasoline
GDI = gasoline direct injection
IC = internal combustion
IMEP = indicated mean effective pressure
M15 = 15% (v/v) methanol blended with 85% (v/v) gasoline
NEDC = New European Driving Cycle
OC = organic carbon
PAH = polycyclic aromatic hydrocarbons
PM = particulate matter
PN = particulate number

REFERENCES

(1) Miyashita, N.; Matsubara, Y.; Iwata, K.; Ishikawa, M. *Spark Plugs for Gasoline Direct Injection Engines*; 0148-7191; SAE Technical Paper, 2001

(2) Zhan, R.; Eakle, S. T.; Weber, P. *Simultaneous reduction of PM, HC, CO and NO_x emissions from a GDI engine*; 0148-7191; SAE Technical Paper, 2010.

(3) Samuel, S.; Hassaneen, A.; Morrey, D. *Particulate matter emissions and the role of catalytic converter during cold start of GDI engine*; 0148-7191; SAE Technical Paper, 2010.

(4) Qin, J.; Li, X.; Pei, Y. *Effects of Combustion Parameters and Lubricating Oil on Particulate Matter Emissions from a Turbo-Charged GDI Engine Fueled with Methanol/Gasoline Blends*; 0148-7191; SAE Technical Paper, 2014.

(5) Whelan, I.; Samuel, S.; Hassaneen, A. *Investigation into the role of catalytic converters on tailpipe-out nano-scale particulate matter from gasoline direct injection engine*; 0148-7191; SAE Technical Paper, 2010.

(6) Stuart, B. O. Deposition and clearance of inhaled particles. *Environ. Health Perspect.* **1984**, *55*, 369.

(7) Chakraborty, A.; Gupta, T. Chemical characterization and source apportionment of submicron (PM1) aerosol in Kanpur region, India. *Aerosol Air Qual. Res.* **2010**, *10* (5), 433−445.

(8) Gupta, T.; Mandariya, A. Sources of submicron aerosol during fog-dominated wintertime at Kanpur. *Environ. Sci. Pollut. Res.* **2013**, *20* (8), 5615−5629.

(9) Oberdörster, G.; Sharp, Z.; Atudorei, V.; Elder, A.; Gelein, R.; Kreyling, W.; Cox, C. Translocation of inhaled ultrafine particles to the brain. *Inhalation Toxicol.* **2004**, *16* (6−7), 437−445.

(10) Geiger, A.; Cooper, J. *Overview of Airborne Metals Regulations, Exposure Limits, Health Effects, and Contemporary Research*; United States Environmental Protection Agency (U.S. EPA): Washington, D.C., 2010.

(11) Choi, K.; Kim, J.; Ko, A.; Myung, C.-L.; Park, S.; Lee, J. Size-resolved engine exhaust aerosol characteristics in a metal foam particulate filter for GDI light-duty vehicle. *J. Aerosol Sci.* **2013**, *57*, 1−13.

(12) Quiros, D. C.; Hu, S.; Hu, S.; Lee, E. S.; Sardar, S.; Wang, X.; Olfert, J. S.; Jung, H. S.; Zhu, Y.; Huai, T. Particle effective density and mass during steady-state operation of GDI, PFI, and diesel passenger cars. *J. Aerosol Sci.* **2015**, *83*, 39−54.

(13) Choi, S.; Seong, H. Oxidation characteristics of gasoline direct-injection (GDI) engine soot: Catalytic effects of ash and modified kinetic correlation. *Combust. Flame* **2015**, *162* (6), 2371−2389.

(14) Bahreini, R.; Xue, J.; Johnson, K.; Durbin, T.; Quiros, D.; Hu, S.; Huai, T.; Ayala, A.; Jung, H. Characterizing emissions and optical properties of particulate matter from PFI and GDI light-duty gasoline vehicles. *J. Aerosol Sci.* **2015**, *90*, 144−153.

(15) An, Y.-z.; Teng, S.-p.; Pei, Y.-q.; Qin, J.; Li, X.; Zhao, H. An experimental study of polycyclic aromatic hydrocarbons and soot emissions from a GDI engine fueled with commercial gasoline. *Fuel* **2016**, *164*, 160−171.

(16) Cucchi, M.; Samuel, S. Influence of the exhaust gas turbocharger on nano-scale particulate matter emissions from a GDI spark ignition engine. *Appl. Therm. Eng.* **2015**, *76*, 167−174.

(17) An, Y.-z.; Pei, Y.-q.; Qin, J.; Zhao, H.; Teng, S.-p.; Li, B.; Li, X. Development of a PAH (polycyclic aromatic hydrocarbon) formation model for gasoline surrogates and its application for GDI (gasoline direct injection) engine CFD (computational fluid dynamics) simulation. *Energy* **2016**, *94*, 367−379.

(18) Yinhui, W.; Rong, Z.; Yanhong, Q.; Jianfei, P.; Mengren, L.; Jianrong, L.; Yusheng, W.; Min, H.; Shijin, S. The impact of fuel compositions on the particulate emissions of direct injection gasoline engine. *Fuel* **2016**, *166*, 543−552.

(19) Wang, C.; Xu, H.; Herreros, J. M.; Wang, J.; Cracknell, R. Impact of fuel and injection system on particle emissions from a GDI engine. *Appl. Energy* **2014**, *132*, 178−191.

DOI: 10.1021/acs.energyfuels.6b02877
Energy Fuels 2017, 31, 4155−4164

(20) Cho, J.; Si, W.; Jang, W.; Jin, D.; Myung, C.-L.; Park, S. Impact of intermediate ethanol blends on particulate matter emission from a spark ignition direct injection (SIDI) engine. *Appl. Energy* **2015**, *160*, 592−602.
(21) Luo, Y.; Zhu, L.; Fang, J.; Zhuang, Z.; Guan, C.; Xia, C.; Xie, X.; Huang, Z. Size distribution, chemical composition and oxidation reactivity of particulate matter from gasoline direct injection (GDI) engine fueled with ethanol-gasoline fuel. *Appl. Therm. Eng.* **2015**, *89*, 647−655.
(22) Wang, X.; Ge, Y.; Liu, L.; Peng, Z.; Hao, L.; Yin, H.; Ding, Y.; Wang, J. Evaluation on toxic reduction and fuel economy of a gasoline direct injection-(GDI-) powered passenger car fueled with methanol−gasoline blends with various substitution ratios. *Appl. Energy* **2015**, *157*, 134−143.
(23) Vancoillie, J.; Demuynck, J.; Sileghem, L.; Van De Ginste, M.; Verhelst, S.; Brabant, L.; Van Hoorebeke, L. The potential of methanol as a fuel for flex-fuel and dedicated spark-ignition engines. *Appl. Energy* **2013**, *102*, 140−149.
(24) Chen, L.; Stone, R.; Richardson, D. A study of mixture preparation and PM emissions using a direct injection engine fuelled with stoichiometric gasoline/ethanol blends. *Fuel* **2012**, *96*, 120−130.
(25) Lattimore, T.; Herreros, J. M.; Xu, H.; Shuai, S. Investigation of compression ratio and fuel effect on combustion and PM emissions in a DISI engine. *Fuel* **2016**, *169*, 68−78.
(26) Köhler, F. *Testing of Particulate Emissions from Positive Ignition Vehicles with Direct Fuel Injection System*; TűV Nord: Hanover, Germany, 2013.
(27) Zhang, H.; Chen, P.; Wang, J.; Wang, Y.-Y. Integrated Study of Inland-Vessel Diesel Engine Two-Cell SCR Systems with Dynamic References. *IEEE/ASME Trans. Mechatronics* **2016**, 1.
(28) Zhang, H.; Wang, J. Adaptive Sliding-Mode Observer Design for A Selective Catalytic Reduction System of Ground-Vehicle Diesel Engines. *IEEE/ASME Trans. Mechatronics* **2016**, *21* (4), 2027−2038.
(29) Zhang, H.; Wang, J.; Wang, Y.-Y. Optimal dosing and sizing optimization for a ground vehicle diesel engine two-cell selective catalytic reduction system. *IEEE Trans. Veh. Technol.* **2016**, *65* (6), 4740−4751.
(30) Price, P.; Twiney, B.; Stone, R.; Kar, K.; Walmsley, H. *Particulate and hydrocarbon emissions from a spray guided direct injection spark ignition engine with oxygenate fuel blends*; 0148-7191; SAE Technical Paper, 2007.
(31) Gao, Y.; Duan, A.; Liu, S.; Wu, X.; Liu, W.; Li, M.; Chen, S.; Wang, X.; Weng, D. Study of $Ag/Ce_xNd_{1-x}O_2$ nanocubes as soot oxidation catalysts for gasoline particulate filters: Balancing catalyst activity and stability by Nd doping. *Appl. Catal., B* **2017**, *203*, 116−126.
(32) Hernández, W.; Tsampas, M.; Zhao, C.; Boreave, A.; Bosselet, F.; Vernoux, P. La/Sr-based perovskites as soot oxidation catalysts for Gasoline Particulate Filters. *Catal. Today* **2015**, *258*, 525−534.
(33) Mamakos, A.; Steininger, N.; Martini, G.; Dilara, P.; Drossinos, Y. Cost effectiveness of particulate filter installation on Direct Injection Gasoline vehicles. *Atmos. Environ.* **2013**, *77*, 16−23.
(34) Ito, Y.; Shimoda, T.; Aoki, T.; Yuuki, K.; Sakamoto, H.; Kato, K.; Thier, D.; Kattouah, P.; Ohara, E.; Vogt, C. *Next Generation of Ceramic Wall Flow Gasoline Particulate Filter with Integrated Three Way Catalyst*; 0148-7191; SAE Technical Paper, 2015.
(35) Ogyu, K.; Ogasawara, T.; Nagatsu, Y.; Yamamoto, Y.; Higuchi, T.; Ohno, K. *Feasibility Study on the Filter Design of Re-Crystallized SiC-GPF for TWC Coating Application*; 0148-7191; SAE Technical Paper, 2015.
(36) Mamakos, A.; Steininger, N.; Martini, G.; Dilara, P.; Drossinos, Y. Cost effectiveness of particulate filter installation on Direct Injection Gasoline vehicles. *Atmos. Environ.* **2013**, *77*, 16−23.
(37) International Organization for Standardization (ISO). *Reciprocating Internal Combustion Engines—Exhaust Emission Measurement—Part 4: Steady-State Test Cycles for Different Engine Applications*; ISO: Geneva, Switzerland, 2007; ISO 8178-4:2007.
(38) Nash, H.; Sly, P. D. Asthma, allergy, and the environment. In *Textbook of Children's Environmental Health*; Landrigan, P., Etzel, R., Eds.; Oxford University Press: New York, 2014; DOI: 10.1093/med/9780199929573.003.0043.
(39) Raizenne, M.; Neas, L. M.; Damokosh, A. I.; Dockery, D. W.; Spengler, J. D.; Koutrakis, P.; Ware, J. H.; Speizer, F. E. Health effects of acid aerosols on North American children: pulmonary function. *Environ. Health Perspect.* **1996**, *104* (5), 506.
(40) Braun-Fahrländer, C.; Vuille, J.; Sennhauser, F.; Neu, U.; Künzle, T.; Grize, L.; Gassner, M.; Minder, C.; Schindler, C.; Varonier, H.; Wüthrich, B. Respiratory health and long term exposure to air pollutants in Swiss schoolchildren. *Am. J. Respir. Crit. Care Med.* **1997**, *155* (3), 1042.
(41) Pierse, N.; Rushton, L.; Harris, R. S.; Kuehni, C. E.; Silverman, M.; Grigg, J. Locally generated particulate pollution and respiratory symptoms in young children. *Thorax* **2006**, *61* (3), 216−220.
(42) Schikowski, T.; Sugiri, D.; Ranft, U.; Gehring, U.; Heinrich, J.; Wichmann, H.-E.; Krämer, U. Long-term air pollution exposure and living close to busy roads are associated with COPD in women. *Respir. Res.* **2005**, *6* (1), 1.
(43) Hora, T. S.; Shukla, P. C.; Agarwal, A. K. Particulate emissions from hydrogen enriched compressed natural gas engine. *Fuel* **2016**, *166*, 574−580.
(44) Wang, X.; Grose, M. A.; Caldow, R.; Osmondson, B. L.; Swanson, J. J.; Chow, J. C.; Watson, J. G.; Kittelson, D. B.; Li, Y.; Xue, J.; Jung, H.; Hu, S. Improvement of Engine Exhaust Particle Sizer (EEPS) size distribution measurement—II. Engine exhaust particles. *J. Aerosol Sci.* **2016**, *92*, 83−94.
(45) Sudrajad, A.; Yusof, A. F. Review of Electrostatic Precipitator Device for Reduce of Diesel Engine Particulate Matter. *Energy Procedia* **2015**, *68*, 370−380.
(46) Sharma, N.; Agarwal, A. K. *Microscopic and Macroscopic Spray Characteristics of GDI Injector Using Gasohol Fuels at Various Injection Pressures*; 0148-7191; SAE Technical Paper, 2016.
(47) Sharma, N.; Agarwal, A. K. *An Experimental Study of Microscopic Spray Characteristics of a GDI Injector Using Phase Doppler Interferometry*; 0148-7191; SAE Technical Paper, 2016.
(48) Agarwal, A. K.; Gupta, T.; Shukla, P. C.; Dhar, A. Particulate emissions from biodiesel fuelled CI engines. *Energy Convers. Manage.* **2015**, *94*, 311−330.
(49) Heywood, J. B. *Internal Combustion Engine Fundamentals*; McGraw-Hill: New York, 1988; Vol. *930*.
(50) Reddy, M. S.; Sharma, N.; Agarwal, A. K. Effect of straight vegetable oil blends and biodiesel blends on wear of mechanical fuel injection equipment of a constant speed diesel engine. *Renewable Energy* **2016**, *99*, 1008−1018.
(51) Wang, Y.; Liang, X.; Shu, G.; Dong, L. Impact of Lubricating Oil on Morphology of Particles from a Diesel Engine. *Energy Procedia* **2015**, *75*, 2388−2393.

DOI: 10.1021/acs.energyfuels.6b02877
Energy Fuels 2017, 31, 4155−4164